DOI: 10.17344/acsi.2020.5895 *Acta Chim. Slov.* **2020,** *67,* 896–903

Scientific paper

Syntheses, Crystal Structures and Catalytic Property of Oxidovanadium(V) Complexes Derived from Tridentate Hydrazone Ligands

Ya-Jun Cai,[1,2] Yuan-Yuan Wu,[1,2] Fei Pan,[1,2] Qi-An Peng[1,2] and Yong-Ming Cui[3,*]

[1] *School of Environmental Engineering, Wuhan Textile University, Wuhan 430073, P. R. China*

[2] *Engineering Research Center for Clean Production of Textile Printing, Ministry of Education, Wuhan 430073, P. R. China*

[3] *National Local Joint Engineering Laboratory for Advanced Textile Processing and Clean Production, Wuhan Textile University, Wuhan 430073, P. R. China*

** Corresponding author: E-mail: fcym981248@sohu.com*

Received: 02-08-2020

Abstract

Two new ethyl maltolato coordinated mononuclear oxidovanadium(V) complexes [VOL^a(emt)]·DMF (**1**) and [VOL^b(emt)] (**2**), where H_2L^a = *N*'-(4-bromo-2-hydroxybenzylidene)-3-hydroxybenzohydrazide, H_2L^b = *N*'-(4-bromo-2-hydroxybenzylidene)benzohydrazide, Hemt = ethyl maltol, have been synthesized and characterized on the basis of CHN elemental analysis, FT-IR and UV-Vis spectroscopy and powder XRD analysis. Structures of the complexes were further characterized by single crystal X-ray diffraction, which indicated that the V atoms in the complexes adopt octahedral coordination. The hydrazones behave as NOO tridentate ligands. The catalytic epoxidation properties on cyclooctene of the complexes were investigated.

Keywords: Hydrazone; oxidovanadium complex; crystal structure; catalytic epoxidation

1. Introduction

Schiff bases are interesting ligands in the formation of versatile complexes with various metal ions.[1] The complexes with Schiff base ligands have received particular attention for their facile synthesis and remarkable biological, catalytic and magnetic applications.[2] Catalytic epoxidation of olefins is an important type of reactions in industrial chemistry. A number of complexes with transition metal ions are active catalysts for this process.[3] In particular, among the complexes, vanadium and molybdenum complexes seem more interesting because of their excellent catalytic ability in the oxidation of olefins and sulfides.[4] Vanadium complexes with hydrazones are reported to possess catalytic properties. In order to study the influence of the substituent groups of the hydrazones on the catalytic property of the vanadium complexes, in this paper, two new oxidovanadium(V) complexes, [VOL^a(emt)]·DMF

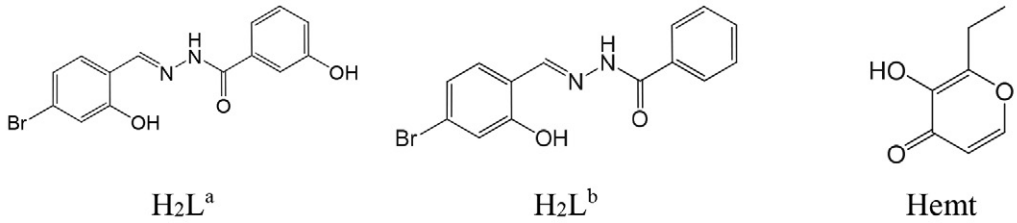

H_2L^a H_2L^b Hemt

Scheme 1. The hydrazones and Hemt.

(**1**) and [VOL^b(emt)] (**2**), where H_2L^a = *N*'-(4-bromo-2-hydroxybenzylidene)-3-hydroxybenzohydrazide, H_2L^b = *N*'-(4-bromo-2-hydroxybenzylidene)benzohydrazide, Hemt = ethyl maltol (Scheme 1), are presented.

2. Experimental

2. 1. Materials and Methods

3-Hydroxybenzohydrazide, benzohydrazide, 4-bromosalicylaldehyde, ethyl maltol and $VO(acac)_2$ were purchased from Alfa Aesar and used as received. Reagent grade solvents were used as received. Microanalyses of the complexes were performed with a Vario EL III CHNOS elemental analyzer. Infrared spectra were recorded as KBr pellets with an FTS-40 spectrophotometer. Electronic spectra were recorded on a Lambda 900 spectrometer. The powder XRD spectra were recorded in a 2θ range of 2–50° using a Bruker D8 Advance detector under ambient conditions. The catalytic reactions were followed by gas chromatography on an Agilent 6890A chromatograph equipped with an FID detector and a DB5-MS capillary column (30 m × 0.32 mm, 0.25 μm). Molar conductance measurements were made by means of a Metrohm 712 conductometer in acetonitrile.

2. 2. Synthesis of the Complex [VOL^a(emt)]·DMF

3-Hydroxybenzohydrazide (10 mmol, 1.52 g) and 4-bromosalicylaldehyde (10 mmol, 2.01 g) were refluxed in methanol (50 mL). Then, $VO(acac)_2$ (10 mmol, 2.63 g) and ethyl maltol (10 mmol, 1.40 g) dissolved in methanol (30 mL) were added to the mixture and refluxed for 1 h in oil bath to give a deep brown solution with some insoluble substance. Then, a few drops of DMF were added until the insoluble substance dissolved. Single crystals of the complex were formed during slow evaporation of the reaction mixture in air. The crystals were isolated by filtration, washed with cold methanol and dried over anhydrous $CaCl_2$. Yield: 0.38 g (61%). IR data (KBr pellet, cm^{-1}): 1667 ν(C=O), 1592 ν(C=N), 1524, 1455, 1408, 1353, 1250 ν(C–$O_{phenolate}$), 1188 ν(N–N), 1107, 1066, 1030, 973 ν(V=O), 926, 850, 796, 727, 630, 522, 468. UV-Vis data in methanol (nm): 210, 269, 320, 398. Molar conductance (10^{-3} mol L^{-1}, methanol): 25 Ω^{-1} cm^2 mol^{-1}. Analysis: Found: C 46.89, H 3.85, N 6.77%. Calculated for $C_{24}H_{23}BrN_3O_8V$: C 47.08, H 3.79, N 6.86%.

2. 3. Synthesis of the Complex [VOL^b(emt)]

Benzohydrazide (10 mmol, 1.36 g) and 4-bromosalicylaldehyde (10 mmol, 2.01 g) were refluxed in methanol (50 mL). Then, $VO(acac)_2$ (10 mmol, 2.63 g) and ethyl maltol (10 mmol, 1.40 g) dissolved in methanol (30 mL) were added to the mixture and refluxed for 1 h in oil bath to give a deep brown solution. Single crystals of the complex were formed during slow evaporation of the reaction mixture in air. The crystals were isolated by filtration, washed with cold methanol and dried over anhydrous $CaCl_2$. Yield: 0.21 g (40%). IR data (KBr pellet, cm^{-1}): 1595 ν(C=N), 1529, 1458, 1407, 1338, 1252 ν(C–$O_{phenolate}$), 1196 ν(N–N), 1131, 1070, 973 ν(V=O), 919, 835, 786, 695, 639, 598, 515, 466. UV-Vis data in methanol (nm): 210, 267, 322, 396. Molar conductance (10^{-3} mol L^{-1}, methanol): 33 Ω^{-1} cm^2 mol^{-1}. Analysis: Found: C 48.37, H 3.16, N 5.22%. Calculated for $C_{21}H_{16}BrN_2O_6V$: C 48.21, H 3.08, N 5.35%.

2. 4. Crystal Structure Determination

Data were collected on a Bruker SMART 1000 CCD area diffractometer using a graphite monochromator Mo Kα radiation (λ = 0.71073 Å) at 298(2) K. The data were corrected with SADABS programs and refined on F^2 with Siemens SHELXL software.[5] The structures of the complexes were solved by direct methods and difference Fourier syntheses. All non-hydrogen atoms were refined anisotropically. The hydrogen atoms were placed in calculated positions and included in the last cycles of refinement. Crystal data and details of the data collection and refinement are listed in Table 1. Selected coordinate bond lengths and angles are listed in Table 2.

Table 1. Crystallographic data for the complexes

Parameters	1	2
Empirical formula	$C_{24}H_{23}BrN_3O_8V$	$C_{21}H_{16}BrN_2O_6V$
Formula weight	612.30	523.21
Crystal system	Triclinic	Monoclinic
Space group	*P*–1	$P2_1/n$
a [Å]	10.0508(11)	12.2708(11)
b [Å]	11.6192(12)	7.4066(7)
c [Å]	12.8769(12)	22.6657(12)
α [°]	63.7350(10)	90
β [°]	68.8460(10)	94.5300(10)
γ [°]	86.6150(10)	90
V [Å^3]	1248.5(2)	2053.5(3)
Z	2	4
$\rho_{calcd.}$ [g cm^{-3}]	1.629	1.692
μ [mm^{-1}]	2.052	2.471
F(000)	620	1048
Measured reflections	27647	11744
Independent reflections	4646	3809
Observed reflections ($I > 2\sigma(I)$)	3541	2765
Parameters	338	281
Restraints	0	0
Final R indices [$I > 2\sigma(I)$]	0.0491, 0.1387	0.0385, 0.0914
R indices (all data)	0.0674, 0.1518	0.0632, 0.1020
Goodness-of-fit on F^2	1.037	1.030
Largest difference in peak and hole (e Å^{-3})	0.941, –0.696	0.542, –0.482

Table 2. Selected bond lengths (Å) and angles (°) for the complexes

1			
V1–O1	1.843(3)	V1–O2	1.918(3)
V1–O4	1.585(3)	V1–O5	2.263(3)
V1–O6	1.862(2)	V1–N1	2.094(3)
O4–V1–O1	100.49(16)	O4–V1–O6	100.18(12)
O1–V1–O6	95.62(11)	O4–V1–O2	94.89(14)
O1–V1–O2	155.78(12)	O6–V1–O2	99.96(11)
O4–V1–N1	101.11(12)	O1–V1–N1	83.47(12)
O6–V1–N1	158.50(11)	O2–V1–N1	75.24(11)
O4–V1–O5	174.17(14)	O1–V1–O5	85.16(13)
O6–V1–O5	77.68(10)	O2–V1–O5	80.23(11)
N1–V1–O5	80.84(10)		
2			
V1–O1	1.849(2)	V1–O2	1.922(2)
V1–O3	1.588(2)	V1–O4	1.872(2)
V1–O5	2.255(2)	V1–N1	2.083(2)
O3–V1–O1	99.32(12)	O3–V1–O4	98.75(11)
O1–V1–O4	102.31(9)	O3–V1–O2	99.79(11)
O1–V1–O2	153.12(10)	O4–V1–O2	93.26(9)
O3–V1–N1	98.47(11)	O1–V1–N1	83.71(9)
O4–V1–N1	160.56(10)	O2–V1–N1	74.93(9)
O3–V1–O5	176.08(11)	O1–V1–O5	83.49(10)
O4–V1–O5	77.91(9)	O2–V1–O5	78.47(9)
N1–V1–O5	84.52(9)		

2. 5. Catalytic Epoxidation Process

A mixture of cyclooctene (2.76 mL, 20 mmol), acetophenone (internal reference) and the complex as the catalyst (0.05 mmol) was stirred and heated up to 80 °C before addition of aqueous *tert*-butyl hydroperoxide (TBHP; 70% w/w, 5.48 mL, 40 mmol). The mixture is initially an emulsion, but two phases become clearly visible as the reaction progresses, a colorless aqueous one and a yellowish organic one. The reaction was monitored for 5 h with withdrawal and analysis of organic phase aliquots (0.1 mL) at required times. Each withdrawn sample was mixed with 2 mL of diethylether, treated with a small quantity of MnO_2 and then filtered through silica and analyzed by GC.

3. Results and Discussion

3. 1. Synthesis

The hydrazone compounds and the complexes were synthesized in a facile and analogous way (Scheme 2).

The hydrazones H_2L^a and H_2L^b act as tridentate dianionic NOO donor ligands toward the VO^{3+} cores. The two complexes were obtained from refluxing mixtures of the hydrazones with $VO(acac)_2$ in 1:1 molar proportion in the presence of ethyl maltol in methanol. Complex **1** is not soluble well in methanol, so DMF was added to improve the solubility. The complexes were isolated as single crystals from

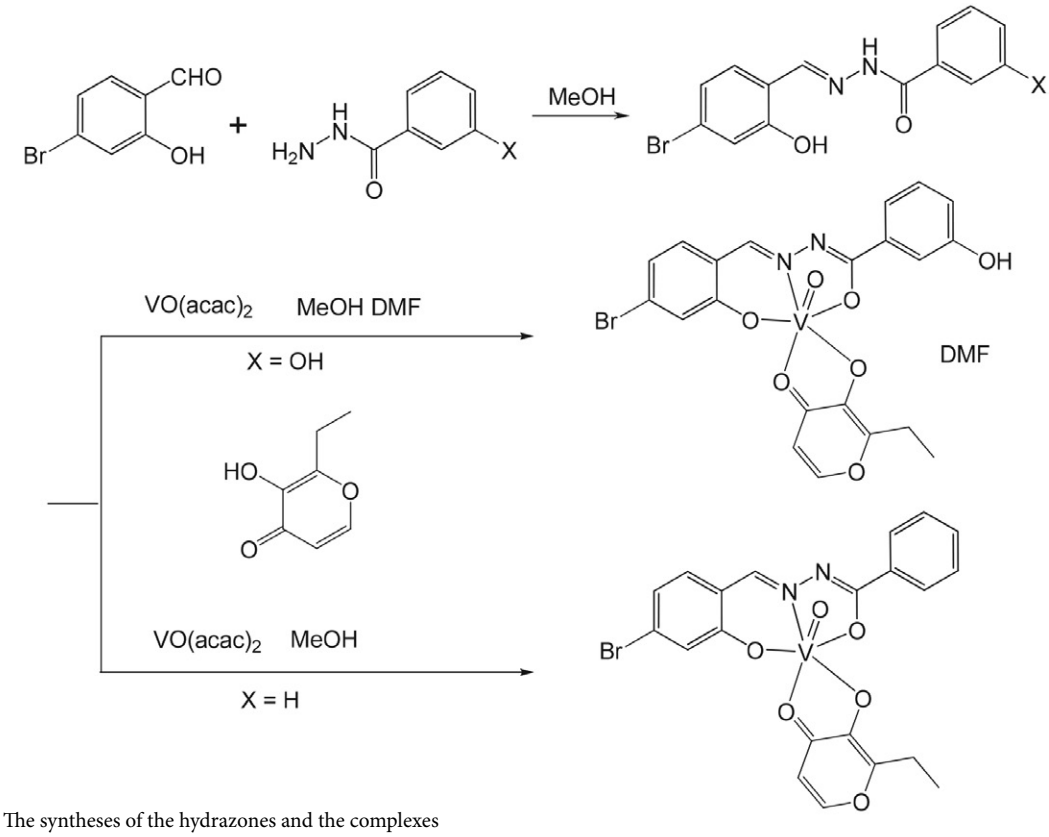

Scheme 2. The syntheses of the hydrazones and the complexes

the reaction mixtures by slow evaporation at room temperature. Crystals of the complexes are stable at room temperature. The low molar solution conductance of the complexes in methanol indicates their non-electrolyte behavior.

Theoretical diffractograms were calculated using the PowderCell program.[6] The experimental X-ray powder diffraction patterns of the bulk samples of the complexes agree well with the simulated patterns calculated from single crystal X-ray diffraction (Figures 1 and 2). The results prove the purity of the bulk samples.

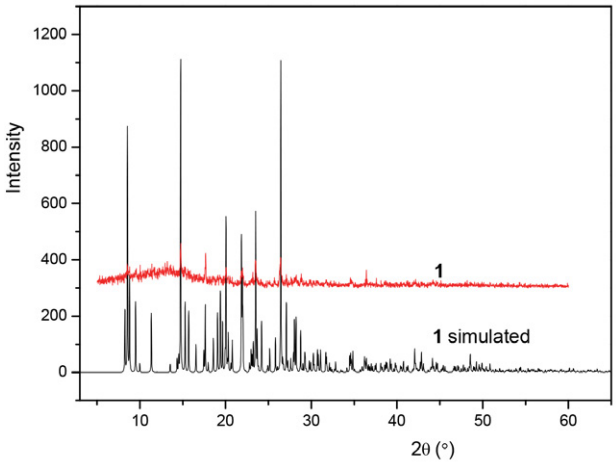

Figure 1. Experimental and simulated powder XRD patterns of complex **1**.

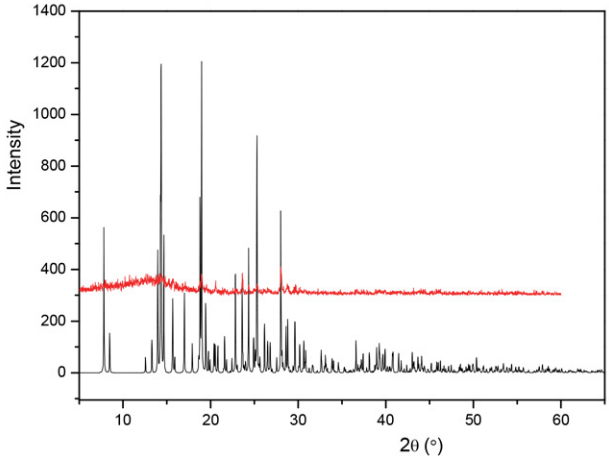

Figure 2. Experimental and simulated powder XRD patterns of complex **2**.

3. 2. IR and Electronic Spectra

The IR spectra of the hydrazones show bands centered at about 3215 cm^{-1} for ν(N–H), 3537 cm^{-1} for ν(O–H), and 1655 cm^{-1} for ν(C=O).[7] The peaks attributed to ν(N–H) and ν(C=O) are absent in the spectra of the complexes as the ligands bind in dianionic form resulting in losing proton from carbohydrazide group. An intense band at 1667 cm^{-1} for complex **1** ascribes to the C=O band of DMF molecule. Strong bands observed at 1592 and 1595 cm^{-1} for the vanadium complexes are attributed to ν(C=N), which are located at lower frequencies as compared to the free hydrazones.[8] The complexes exhibit characteristic bands at 973 cm^{-1} for the stretching of V=O bonds.[9] Based on the IR absorption, it is obvious that the hydrazone ligands exist in the uncoordinated form in *keto*-amino tautomer form and in the complexes in imino-enol tautomeric form. This is not uncommon in the coordination of the hydrazone compounds.[10] The absorptions at about 1525 and 1460 cm^{-1} are assigned to the ν(C=O) and ν(C=C) of the maltolate groups.[11]

The UV-Vis spectra of the hydrazones and the complexes recorded in methanol are shown in Figures 3 and 4, respectively. The absorptions at about 300 nm for the hydrazones are assigned to the n–π^* transitions. The strong absorption bands centered at about 400 nm for the complexes are assigned as charge transfer transitions of N($p\pi$)–V($d\pi$) LMCT. The medium absorption bands centered at about 320 nm for the complexes are assigned as charge transfer transitions of O($p\pi$)–V($d\pi$) LMCT.[12]

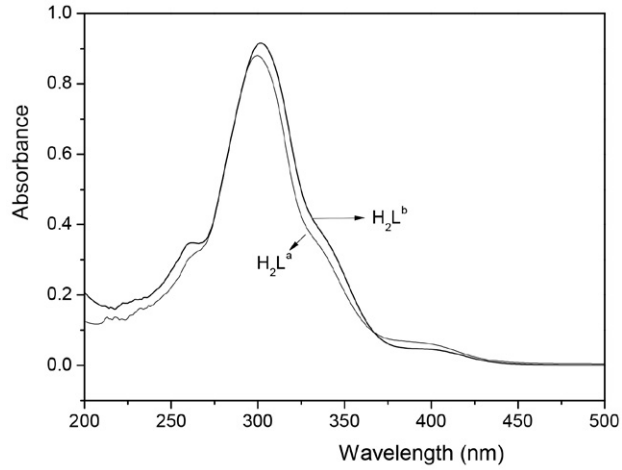

Figure 3. The UV-Vis spectra of H_2L^a and H_2L^b.

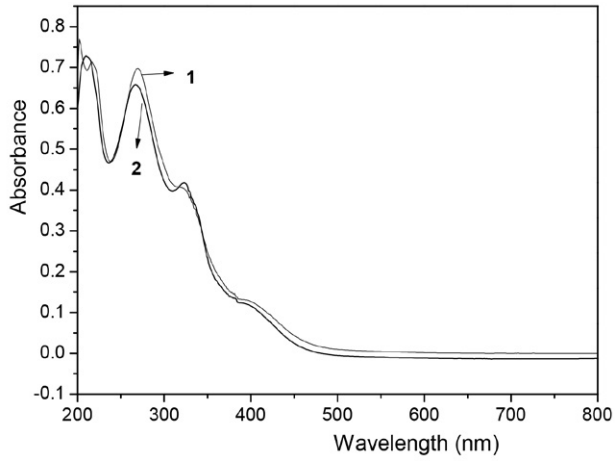

Figure 4. The UV-Vis spectra of complexes **1** and **2**.

3. 3. Description of the Structures of the Complexes

The molecular structures of complexes **1** and **2** are depicted in Figures 5 and 6, respectively. There is a solvated DMF molecule in complex **1**. The V atoms in both complexes are in distorted octahedral coordination with NO_5 chromophore. The dianionic tridentate hydrazones coordinate to the V atoms with the phenolate oxygen (O1), the enolate oxygen (O2) and the imine nitrogen (N1). The emt ligand coordinates to the V atom with the carbonyl oxygen (O5) and phenolate oxygen (O6). The octahedral coordination is defined by the three donor atoms of the hydrazone and the O6 atom at the equatorial plane, and by the oxido oxygen (O4 for **1** and O3 for **2**) and the O5 atom at the axial positions. The V atoms in complex **1** and **2** deviated from the least-squares planes defined by the equatorial donor atoms by 0.306(1) Å and 0.302(1) Å, respectively. The V1–O5 bond lengths (2.26 Å) in both complexes are longer than the remaining V–O bonds (1.58–2.10 Å), which is caused by the *trans* effects generated by the oxido groups. The bond lengths of V–O and V–N are within the values observed in other vanadium(V) complexes.[2f,4e,13] The bond lengths of C8–O2 (1.31 Å) indicate they are more close to single bonds, which is due to the conjugation effects of the ligands.[14] In addition, the bond lengths of C8–N2 (1.30 Å) and N1–N2 (1.40 Å) are intermediate between single and double bonds, which also supports the electron cloud delocalization in the hydrazone ligands. The five-membered chelate rings (V1-N1-N2-C8-O2) are nearly planar, while the six-membered chelate rings (V1-O1-C2-C1-C7-N1) are obviously distorted from planarity. The benzene rings of the hydrazone ligands form dihedral angles of 1.8(3)° (**1**) and 8.7(4)° (**2**). The distortion of the octahedral coordination can be observed from the *trans* angles (157.8(1)–174.2(1)° for **1** and 153.8(1)–176.1(1)° for **2**).

In the crystal structures of complexes **1** and **2** (Figures 7 and 8), the complexes molecules are linked together by hydrogen bonds (Table 3).

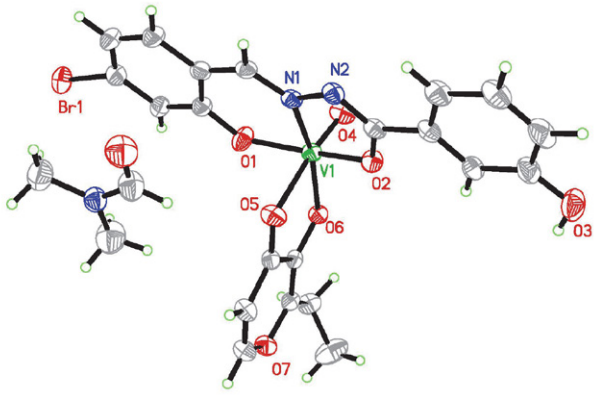

Figure 5. ORTEP plots (30% probability level) and numbering scheme for complex **1**.

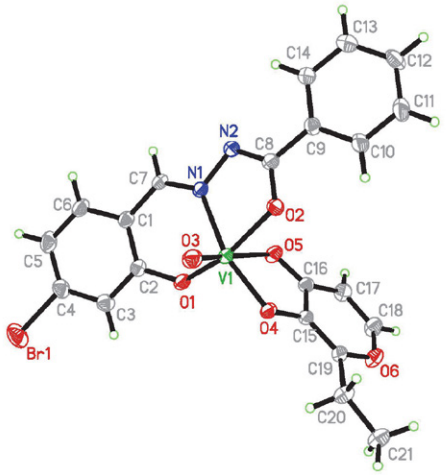

Figure 6. ORTEP plots (30% probability level) and numbering scheme for complex **2**.

3. 4. Catalytic Epoxidation Property

The complexes showed good properties on the cyclooctene epoxidation reaction by using aqueous TBHP as oxidant with no extra addition of organic solvents. Kinetic profiles of complexes **1** and **2** as the catalysts are presented

Table 3. Hydrogen bond distances (Å) and bond angles (°) for the complexes

D–H···*A*	*d*(*D*–H), Å	*d*(H···*A*), Å	*d*(*D*···*A*), Å	Angle (*D*–H···*A*), °
1				
O3–H3···O8^{i}	0.82	1.81	2.628(5)	178(3)
C19–H19···O5^{ii}	0.93	2.51	3.357(5)	151(3)
C20–H20A···O4^{iii}	0.97	2.53	3.264(5)	132(3)
2				
C17–H17···O3^{iv}	0.93	2.48	3.330(5)	153(3)
C21–H21B···O5^{v}	0.96	2.52	3.440(5)	160(3)

Symmetry codes: i) –1 + *x*, *y*, *z*; ii) 1 – *x*, –*y*, 1 – *z*; iii) 1 – *x*, 1 – *y*, –*z*; iv) *x*, 1 + *y*, *z*; v) 2 – *x*, 2 – *y*, –*z*.

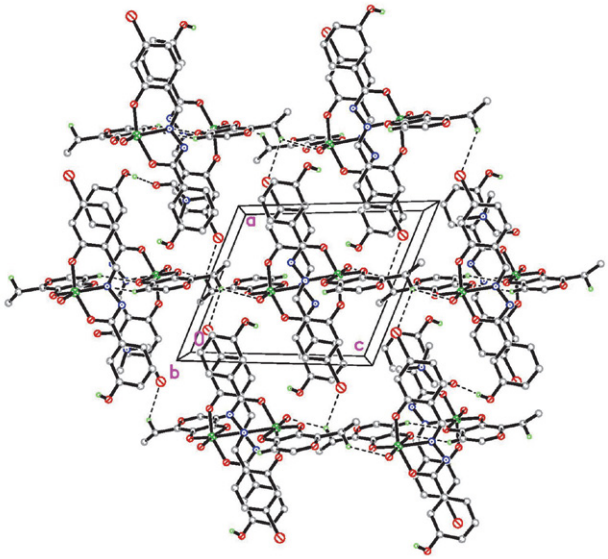

Figure 7. The molecular packing diagram of complex **1**, viewed down the *b* axis. Hydrogen bonds are shown as dashed lines.

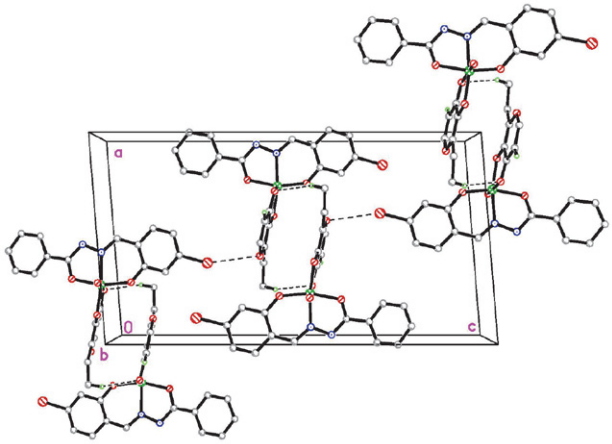

Figure 8. The molecular packing diagram of complex **2**, viewed down the *b* axis. Hydrogen bonds are shown as dashed lines.

in Figure 9. The cyclooctene conversions for complexes **1** and **2** are 91% and 90% after 5 h, and the selectivities for cyclooctene oxide are 67 and 69%. The proposed mechanism is shown in Scheme 3. The TBHP molecule was considered to be coordinated to the V atom with the formation of an O–H···O hydrogen bond. Interestingly, the vanadium complexes in this work have higher conversions and selectivities for the epoxidation reaction of cyclooctene than the molybdenum complexes with hydrazone ligands.[15] From the results, it is not obvious difference between the conversions of the complexes, but the selectivity of complex **2** with benzene as the terminal group of the hydrazone ligand (L^b) is a litter higher than complex **1** with *p*-hydroxylbenzene as the terminal groups of the hydrazone ligand (L^a).

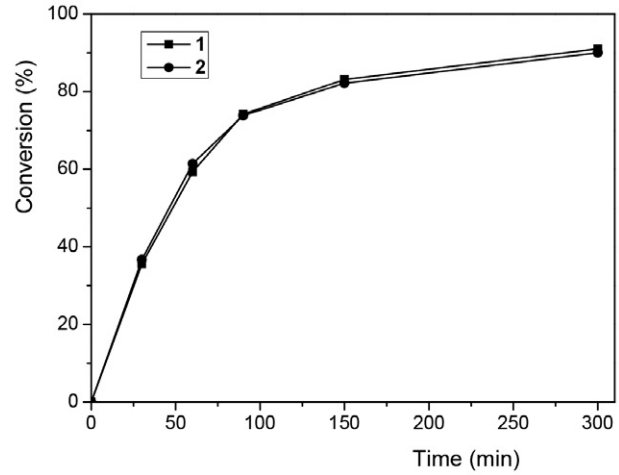

Figure 9. Kinetic monitoring of *cis*-cyclooctene epoxidation with TBHP–H_2O in the presence of the complexes **1** and **2**.

4. Conclusion

In summary, two new structurally similar oxidovanadium(V) complexes derived from the tridentate hydra-

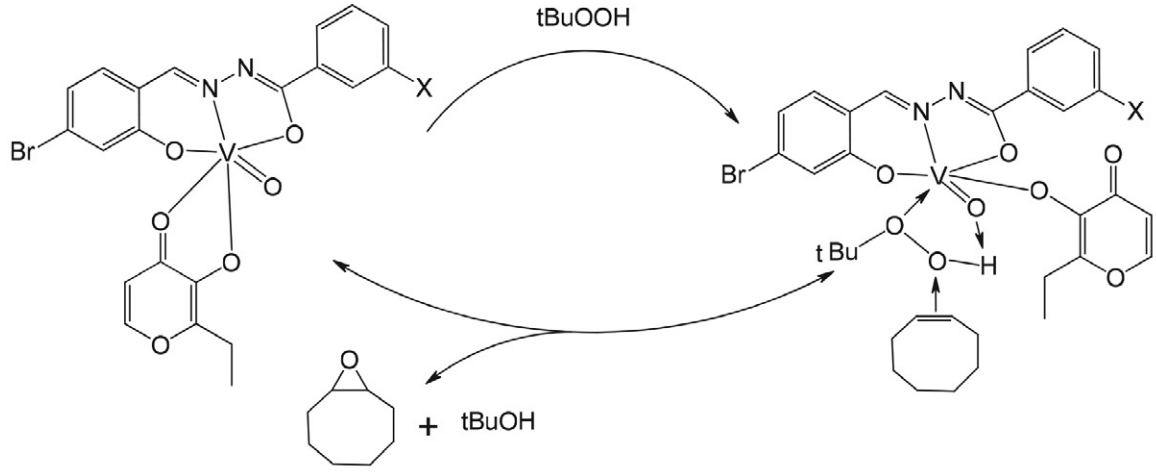

Scheme 3. Proposed mechanism for the catalytic reaction. X = OH for **1**, and X = H for **2**.

zones *N*'-(4-bromo-2-hydroxybenzylidene)-3-hydroxybenzohydrazide and *N*'-(4-bromo-2-hydroxybenzylidene) benzohydrazide, and the bidentate ligand ethyl maltol were prepared and structurally characterized. The hydrazone ligands coordinate to the vanadium atoms through the NOO donor set. The V atoms of the complexes are in octahedral coordination. The ethyl maltol ligand can be substituted by TBHP during the catalytic processes. The complexes have effective catalytic epoxidation properties on cyclooctene with high conversions.

5. Supplementary data

CCDC numbers 1979493 for **1** and 1979494 for **2** contain the supplementary crystallographic data. These data can be obtained free of charge *via* http://www.ccdc.cam.ac.uk/conts/retrieving.html, or from the Cambridge Crystallographic Data Center, 12, Union Road, Cambridge CB2 1EZ, UK; fax: +44 1223 336 033; or e-mail: deposit@ccdc.cam.ac.uk.

Acknowledgments

This work was supported by the Collaborative Innovation Plan of Hubei Province for Key Technology of Eco-Ramie Industry.

6. References

1. (a) S. V. F. Beddoe, R. F. Lonergan, M. B. Pitak, J. R. Price, S. J. Coles, J. A. Kitchen, T. D. Keene, *Dalton Trans.* **2019**, *48*, 15553–15559; **DOI:**10.1039/C9DT01527B
(b) S. Thakur, M. G. B. Drew, A. Franconetti, A. Frontera, S. Chattopadhyay, *RSC Advances* **2019**, *9*, 35165–35175; **DOI:**10.1039/C9RA07006K
(c) H.-Y. Qian, N. Sun, *Transition Met. Chem.* **2019**, *44*, 501–506; **DOI:**10.1007/s11243-018-00296-x
(d) C.-L. Zhang, X.-Y. Qiu, S.-J. Liu, *Acta Chim. Slov.* **2019**, *66*, 484–489; **DOI:**10.17344/acsi.2019.5019
(e) H.-Y. Qian, *Inorg. Nano-Met. Chem.* **2018**, *48*, 615–619; **DOI:**10.1080/24701556.2019.1567542
(f) Y. Li, L. Xu, M. Duan, B. Zhang, Y. Wang, Y. Guan, J. Wu, C. Jing, Z. You, *Polyhedron* **2019**, *166*, 146–152. **DOI:**10.1016/j.poly.2019.03.051
2. (a) T. A. Bazhenova, V. S. Mironov, I. A. Yakushev, R. D. Svetogorov, O. V. Maximova, Y. V. Manakin, A. B. Kornev, A. N. Vasiliev, E. B. Yagubskii, *Inorg. Chem.* **2020**, *59*, 563–578; **DOI:**10.1021/acs.inorgchem.9b02825
(b) H.-Y. Qian, *Inorg. Nano-Met. Chem.* **2018**, *48*, 461–466; **DOI:**10.1080/24701556.2019.1569689
(c) H. Y. Qian, *Russ. J. Coord. Chem.* **2017**, *43*, 780–786; **DOI:**10.1134/S1070328417110070
(d) K. Dankhoff, M. Gold, L. Kober, F. Schmitt, L. Pfeifer, A. Durrmann, H. Kostrhunova, M. Rothemund, V. Brabec, R. Schobert, B. Weber, *Dalton Trans.* **2019**, *48*, 15220–15230; **DOI:**10.1039/C9DT02571E
(e) H. Y. Qian, *Russ. J. Coord. Chem.* **2018**, *44*, 32–38; **DOI:**10.1134/S1070328418010074
(f) M. Duan, Y. Li, L. Xu, H. Yang, F. Luo, Y. Guan, B. Zhang, C. Jing, Z. You, *Inorg. Chem. Commun.* **2019**, *100*, 27–31; **DOI:**10.1016/j.inoche.2018.12.009
(g) E. Zarenezhad, S. Esmaielzadeh, *Acta Chim. Slov.* **2018**, *65*, 416–428. **DOI:**10.17344/acsi.2018.4159
3. (a) K. Moghe, A. K. Sutar, I. K. Kang, K. C. Gupta, *RSC Advances* **2019**, *9*, 30823–30834; **DOI:**10.1039/C9RA05811G
(b) G. Tseberlidis, L. Demonti, V. Pirovano, M. Scavini, S. Cappelli, S. Rizzato, R. Vicente, A. Caselli, *ChemCatChem* **2019**, *11*, 4907–4915; **DOI:**10.1002/cctc.201901045
(c) Y. Kobayashi, R. Obayashi, Y. Watanabe, H. Miyazaki, I. Miyata, Y. Suzuki, Y. Yoshida, T. Shioiri, M. Matsugi, *Eur. J. Org. Chem.* **2019**, *13*, 2401–2408; **DOI:**10.1002/ejoc.201900146
(d) X. Engelmann, D. D. Malik, T. Corona, K. Warm, E. R. Farquhar, M. Swart, W. Nam, K. Ray, *Angew. Chem. Int. Ed.* **2019**, *58*, 4012–4016. **DOI:**10.1002/anie.201812758
4. (a) M. Safaiee, M. Moeinimehr, M. A. Zolfigol, *Polyhedron* **2019**, *170*, 138–150; **DOI:**10.1016/j.poly.2019.05.007
(b) R. J. Comito, Z. W. Wu, G. H. Zhang, J. A. Lawrence, M. D. Korzynski, J. A. Kehl, J. T. Miller, M. Dinca, *Angew. Chem. Int. Ed.* **2018**, *57*, 8135–8139; **DOI:**10.1002/anie.201803642
(c) H. Hayashibara, X. H. Hou, K. Nomura, *Chem. Commun.* **2018**, *54*, 13559–13562; **DOI:**10.1039/C8CC07974A
(d) M. Q. E. Mubarak, S. P. de Visser, *Dalton Trans.* **2019**, *48*, 16899–16910; **DOI:**10.1039/C9DT03048D
(e) M. Liang, N. Sun, D.-H. Zou, *Acta Chim. Slov.* **2018**, *65*, 964–969; **DOI:**10.17344/acsi.2018.4625
(f) L.-W. Xue, Q.-L. Peng, P.-P. Wang, H.-J. Zhang, *Acta Chim. Slov.* **2019**, *66*, 694–700. **DOI:**10.17344/acsi.2019.5151
5. G. M. Sheldrick, SHELXS97 Program for solution of crystal structures, University of Göttingen, Germany, **1997**.
6. W. Kraus, G. Nolge, PowderCell 2.3, Federal Institute for Materials Research and Testing, Berlin, Germany, **1999**.
7. (a) Y.-T. Ye, F. Niu, Y. Sun, D. Qu, X.-L. Zhao, J. Wang, D.-M. Xian, H. Jurg, Z.-L. You, *Chinese J. Inorg. Chem.* **2015**, *31*, 1019–1026;
(b) Z.-L. You, D.-M. Xian, M. Zhang, *Cryst. Eng. Comm.* **2012**, *14*, 7133–7136. **DOI:**10.1039/c2ce26201k
8. (a) R. A. Lal, M. Chakrabarty, S. Choudhury, A. Ahmed, R. Borthakur, A. Kumar, *J. Coord. Chem.* **2010**, *63*, 163–175; **DOI:**10.1080/00958970903259451
(b) T. Glowiak, L. Jerzykiewicz, J. A. Sobczak, J. J. Ziolkowski, *Inorg. Chim. Acta* **2003**, *356*, 387–392. **DOI:**10.1016/S0020-1693(03)00301-3
9. C. A. Koellner, N. A. Piro, W. S. Kassel, C. R. Goldsmith, C. R. Graves, *Inorg. Chem.* **2015**, *54*, 7139–7141. **DOI:**10.1021/acs.inorgchem.5b01136
10. (a) L.-X. Li, Y. Sun, Q. Xie, Y.-B. Sun, K.-H. Li, W. Li, Z.-L. You, *Chinese J. Inorg. Chem.* **2016**, *32*, 369–376;
(b) L. Pan, C. Wang, K. Yan, K.-D. Zhao, G.-H. Sheng, H.-L. Zhu, X.-L. Zhao, D. Qu, F. Niu, Z.-L. You, *J. Inorg. Biochem.*

2016, *159*, 22–28; **DOI:**10.1016/j.jinorgbio.2016.02.017
(c) D. Qu, F. Niu, X. Zhao, K.-X. Yan, Y.-T. Ye, J. Wang, M. Zhang, Z. You, *Bioorg. Med. Chem.* **2015**, *23*, 1944–1949. **DOI:**10.1016/j.bmc.2015.03.036
11. P. Caravan, L. Gelmini, N. Glover, F. G. Herring, H. Li, J. H. McNeill, S. J. Rettig, I. A. Setyawati, E. Shuter, Y. Sun, A. S. Tracey, V. G. Yuen, C. Orvig, *J. Am. Chem. Soc.* **1995**, *117*, 12759–12770. **DOI:**10.1021/ja00156a013
12. (a) R. Hahn, U. Kusthardt, W. Scherer, *Inorg. Chim. Acta* **1993**, *210*, 177–182; **DOI:**10.1016/S0020-1693(00)83325-3
(b) S. Gupta, A. K. Barik, S. Pal, A. Hazra, S. Roy, R. J. Butcher, S. K. Kar, *Polyhedron* **2007**, *26*, 133–141. **DOI:**10.1016/j.poly.2006.08.001
13. (a) M. R. Maurya, S. Agarwal, C. Bader, M. Ebel, D. Rehder, *Dalton Trans.* **2005**, 537–544;
(b) H.-Y. Qian, *Acta Chim. Slov.* **2019**, *66*, 995–1001; **DOI:**10.4149/neo_2019_190112N36
(c) Y. Li, L. Xu, M. Duan, J. Wu, Y. Wang, K. Dong, M. Han, Z. You, *Inorg. Chem. Commun.* **2019**, *105*, 212–216; **DOI:**10.1016/j.inoche.2019.05.011
(d) L. Xu, Y. Li, M. Duan, Y. Li, M. Han, J. Wu, Y. Wang, K. Dong, Z. You, *Polyhedron* **2019**, *165*, 138–142. **DOI:**10.1016/j.poly.2019.03.016
14. T. M. Asha, M. R. P. Kurup, *Polyhedron* **2019**, *169*, 151–161. **DOI:**10.1016/j.poly.2019.04.045
15. Q. Liu, J. Lin, J. Liu, W. Chen, Y. Cui, *Acta Chim. Slov.* **2016**, *63*, 279–286.

Povzetek

Sintetizirali smo dva nova etil maltolato koordinacijska enojedrna oksidovanadijeva(V) kompleksa [VOL^a(emt)]·DMF (**1**) in [VOL^b(emt)] (**2**), kjer je H_2L^a = *N*'-(4-bromo-2-hidroksibenziliden)-3-hidroksibenzohidrazid, H_2L^b = *N*'-(4-bromo-2-hidroksibenziliden)benzohidrazid, Hemt = etil maltol, ter ju okarakterizirali s CHN elementno analizo, FT-IR in UV-Vis spektroskopijo ter praškovno XRD analizo. Strukture smo določili z monokristalno rentgensko difrakcijo, ki razkrije, da imajo V atomi v kompleksu oktaedrično koordinacijo. Hidrazona sta NOO trivezna liganda. Katalitične lastnostni obeh kompleksov smo raziskali z reakcijo epoksidacije ciklooktena.